

SUPPORTING INFORMATION

Photoluminescence enhancement by controllable aggregation and polymerization of octanuclear gold clusters

Biao Yang, Han Wu, Liang Zhao*

The Key Laboratory of Bioorganic Phosphorus Chemistry & Chemical Biology (Ministry of Education), Department of Chemistry, Tsinghua University, Beijing 100084, China.

E-mail: zhaolchem@mail.tsinghua.edu.cn.

Experimental section

Materials and methods

All commercially available chemicals were used without further purification. The solvents used in this study were dried by standard procedures. $[\text{Au}_8(\text{dppp})_4](\text{NO}_3)_2$ were prepared according to the published methods^[1].

Photophysical measurements.

Luminescence quantum yields for solution samples were measured by the optical dilute method. Luminescent decay experiments and photo-luminescent spectra were measured on an Edinburgh FLS980 spectrometer.

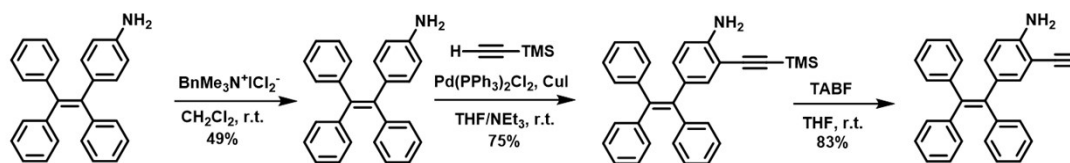
^1H NMR experiments were carried out on a JEOL ECX-400 MHz instrument. Electrospray ionization mass spectrometry (ESI-MS) measurement was carried out on Thermo Fisher Q-Exactive. Elemental analysis was performed on FLASH EA1112. UV-Vis spectra were recorded on a Cary 7000 UV-Vis-NIR spectrophotometer. Transmission electron microscopy (TEM) measurements were performed on Hitachi H-7650 microscope. Liquid tests were carried out by dissolving gold clusters into corresponding solvent. Temperature-dependent PL measurements were carried out in an Edinburgh spectrofluorimeter (FLS980). The fluorimeter is coupled with an Optistat DN cryostat (Oxford Instruments), and the ITC temperature controller and a pressure gauge were used to conduct the temperature-dependent experiments from 77K to 297 K. Spectra were taken at different temperatures after a wait period of 10 min. The error in temperature setting is ± 2 K. The PL quantum yields were obtained by relative methods using rhodamine B as a standard. Luminescent decay experiments were measured on an Edinburgh FLS980 spectrometer using time-correlated single photon counting (TCSPC). Decay in the PL intensity (I) with time (t) was fitted by a double-exponential function:

$$I = A_1 e^{-t/\tau_1} + A_2 e^{-t/\tau_2} + A_3 e^{-t/\tau_3}$$

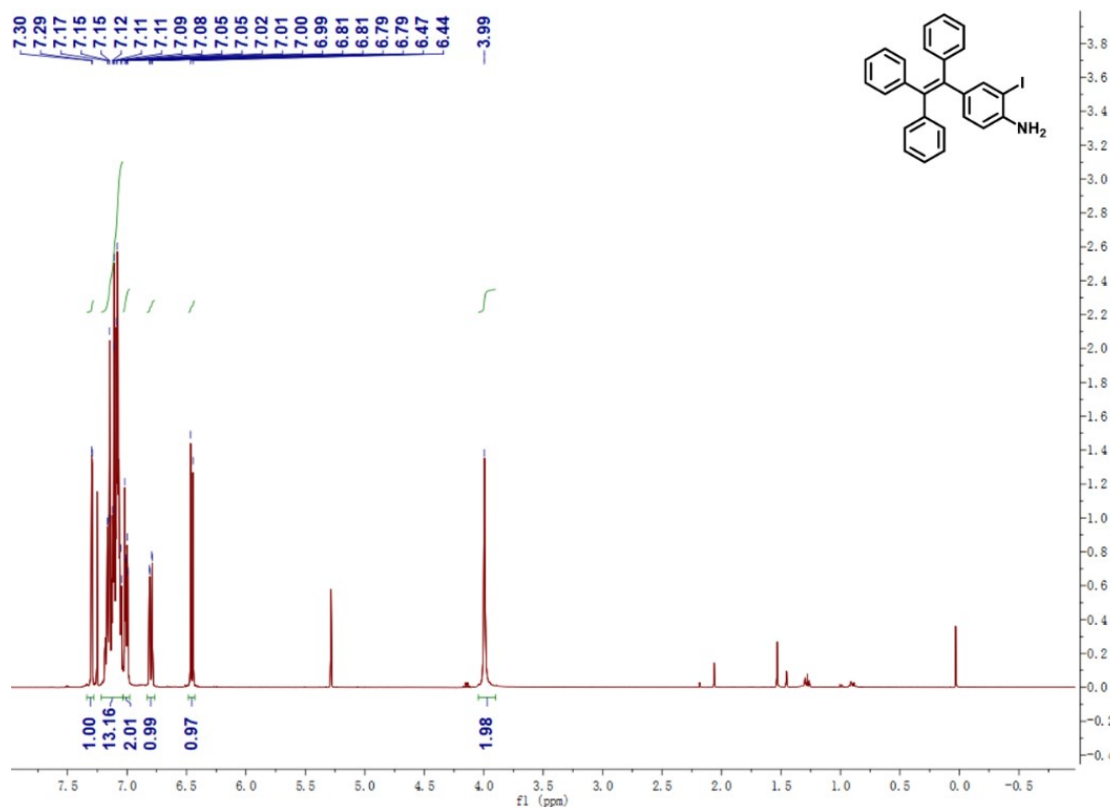
DOSY experiments were carried out on a Bruker Avance 600 MHz instrument using a 5mm TXI HC/N Z-GRD probe. 2D sequence for diffusion measurements were conducted using stimulated echo and LED with 2 spoil gradients. All ^1H -DOSY spectra were recorded at 298 K with 50 ms diffusion delay, 16 squared increments for gradient levels and 32 transients. Gradient strength was set as 50 G/cm. Molecular sizes of 1 and 2-(S) in CD_3OD were calculated according to the Einstein-Stokes equation:

$$D = \frac{k_B T}{6\pi\eta r}$$

T : temperature (K); η : viscosity constant of DMSO = 2.0×10^{-3} Pas, viscosity constant of CD_2Cl_2 = 4.4×10^{-4} Pas; k_B : Boltzmann's constant; D : diffusion coefficient; r : radius of the spherical particle.



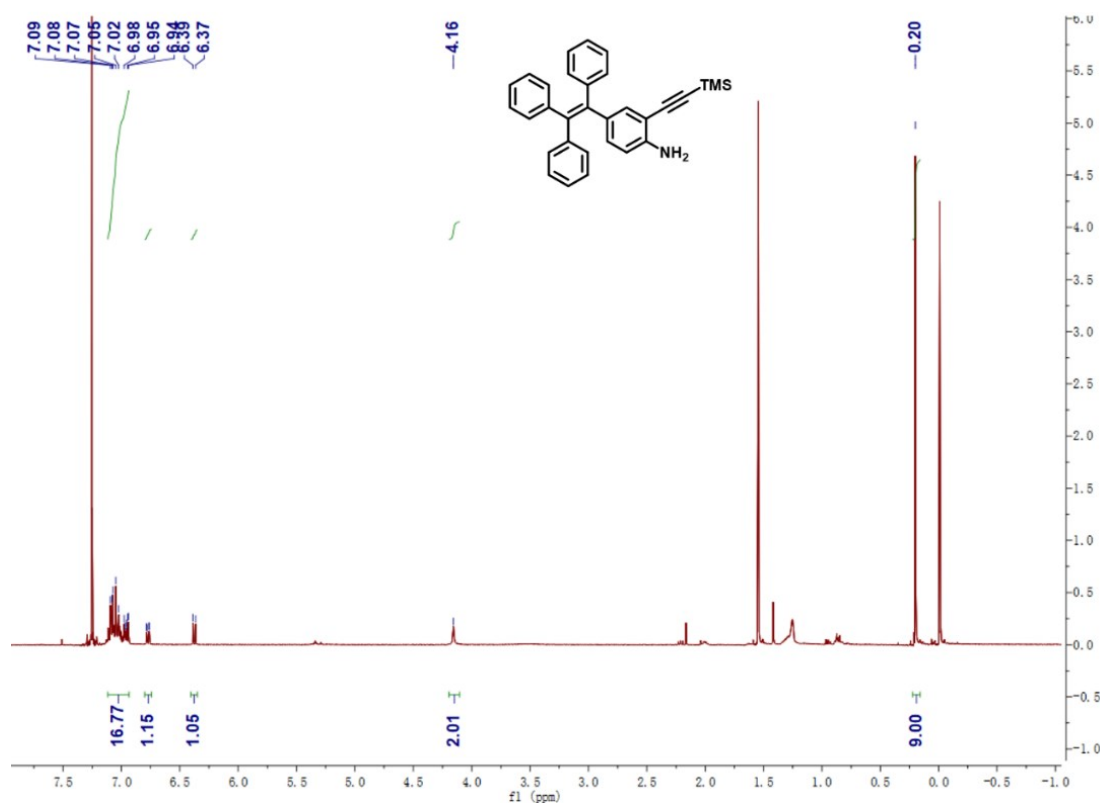
Synthesis of 4-(1,2,2-triphenylethenyl)-2-iodophenylamine. To a stirred solution of 4-(1,2,2-triphenylethenyl)-benzenamine (694 mg, 2 mmol) and CaCO_3 (400 mg, 4 mmol) in CH_2Cl_2 (10 mL) and MeOH (4 mL) was added benzyltrimethylammonium dichloroiodate (696 mg, 2 mmol) at 0 °C. The reaction mixture was stirred at room temperature for 6 h. The mixture was then quenched with saturated NaHCO_3 and saturated Na_2SO_3 at 0 °C and extracted with CH_2Cl_2 . The combined organic layers were washed with brine, dried over Na_2SO_4 and concentrated. The residue was purified by flash column chromatography on silica gel (petroleum ether/ethyl acetate = 30:1 as eluent) to afford 4-(1,2,2-triphenylethenyl)-2-iodophenylamine. Yield: 49%. ^1H NMR (400 MHz, CDCl_3) δ 7.30 (d, 1H), 7.17-7.02(m, 13H), 7.05 (m, 2H), 6.80 (dd, 1H), 6.45 (d, 1H), 3.99 (s, 2H).



^1H NMR spectrum (400 MHz, CDCl_3 , 298K) of 4-(1,2,2-triphenylethenyl)-2-iodophenylamine

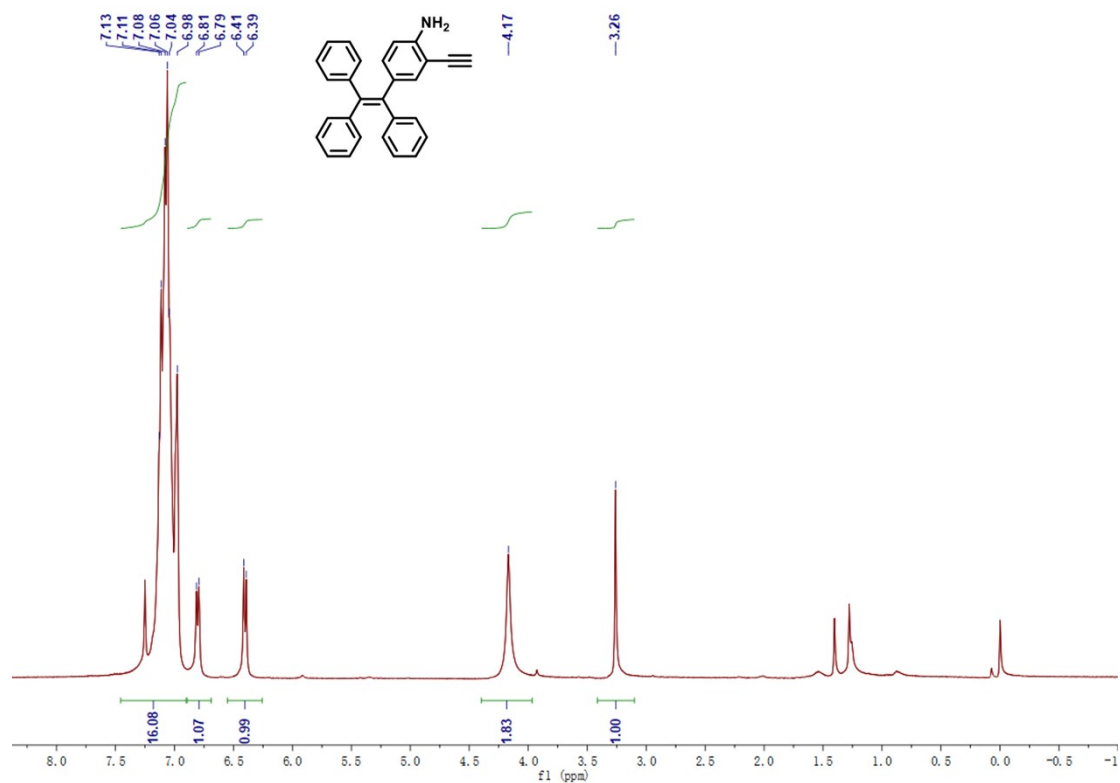
Synthesis of 2-(trimethylsilyl)ethynyl-4-(1,2,2-triphenylethenyl)-phenylamine. To a stirred mixture of 4-(1,2,2-triphenylethenyl)-2-iodophenylamine (237 mg, 0.5 mmol), $\text{PdCl}_2(\text{PPh}_3)_2$ (7 mg, 2 mol %) and CuI (3.8 mg, 4 mol %) in Et_3N (5 mL) and THF (10 mL) at room temperature under an argon atmosphere, trimethylsilylacetylene (0.14 mL, 1.0 mmol, 2 equiv.) was added dropwise. The reaction mixture was stirred for 12 h at

room temperature. The reaction mixture was filtered through Celite and the solvent was removed by rotary evaporation. The residue was treated with water and extracted with CH₂Cl₂. The combined organic phases was washed with brine, dried over anhydrous Na₂SO₄ and the solvent was removed under vacuum. The residue was purified by flash column chromatography on silica gel (petroleum ether/ethyl acetate = 40:1 as eluent) to afford 2-(trimethylsilyl)ethynyl-4-(1,2,2-triphenylethenyl)-phenylamine. Yield: 75%. ¹H NMR (400 MHz, CDCl₃) δ 7.09-6.94 (m, 15H), 6.77 (dd, 1H), 6.38 (d, 1H), 4.16 (s, 2H), 0.20 (s, 9H).

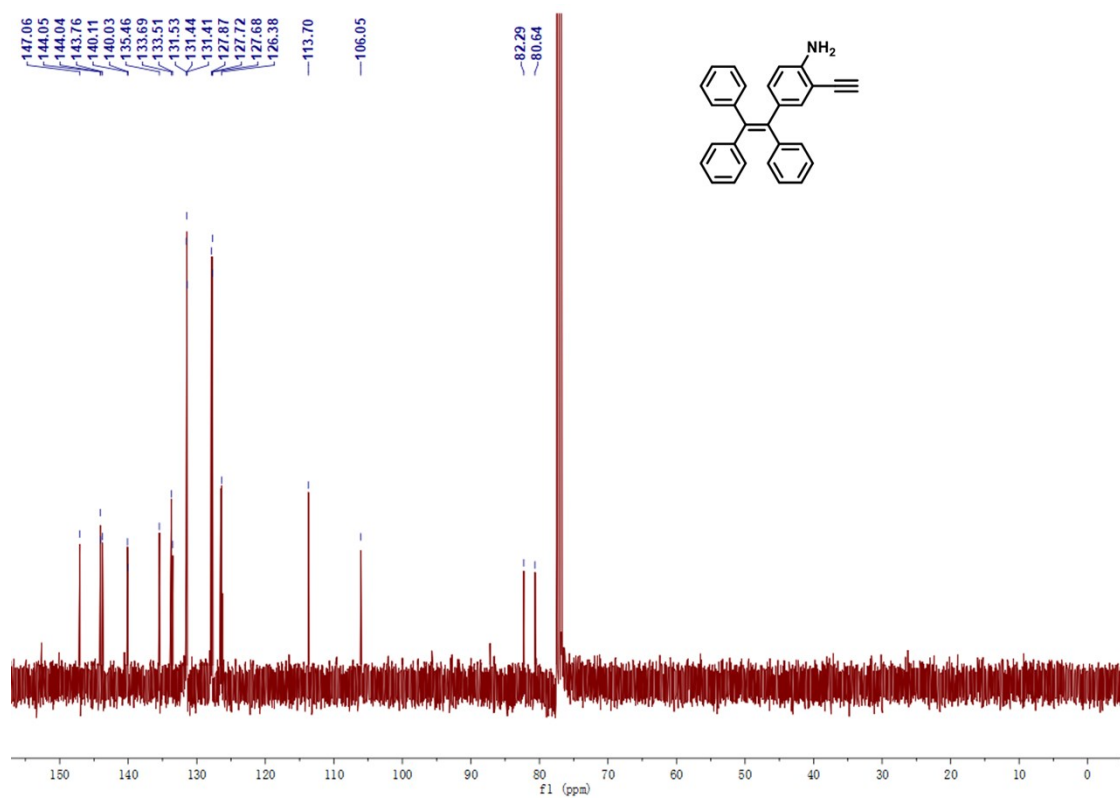


¹H NMR spectrum (400 MHz, CDCl₃, 298K) of 4-(1,2,2-triphenylethenyl)-2-iodophenylamine.

Synthesis of 4-(1,2,2-triphenylethenyl)-phenylamine-2-ethynide (o-TPEA). 2-(trimethylsilyl)ethynyl-4-(1,2,2-triphenylethenyl)-phenylamine (177 mg, 0.4 mmol) and tetrabutylammonium fluoride (1.0 M THF solution, 0.8 mL, 0.8 mmol) were mixed together in THF (40 mL). The solution was left under stirring for 2 h at room temperature. Then it was hydrolyzed with water (10 mL) and extracted with CH₂Cl₂. The combined organic phases were washed with brine, dried over anhydrous Na₂SO₄ and the solvent was removed under vacuum. The residue was purified by flash column chromatography on silica gel (petroleum ether/ethyl acetate = 20:1 as eluent) to afford o-TPEA. Yield: 83%. ¹H NMR (400 MHz, CDCl₃) δ 7.30 (d, 1H), 7.17-7.02(m, 13H), 7.05 (m, 2H), 6.80 (dd, 1H), 6.45 (d, 1H), 3.99 (s, 2H). ¹³C NMR (100 MHz, CDCl₃) δ 147.06, 144.05, 144.04, 143.76, 140.11, 140.03, 135.46, 133.69, 133.51, 131.53, 131.44, 131.41, 127.87, 127.72, 127.68, 126.38, 113.70, 106.05, 82.29, 80.64.

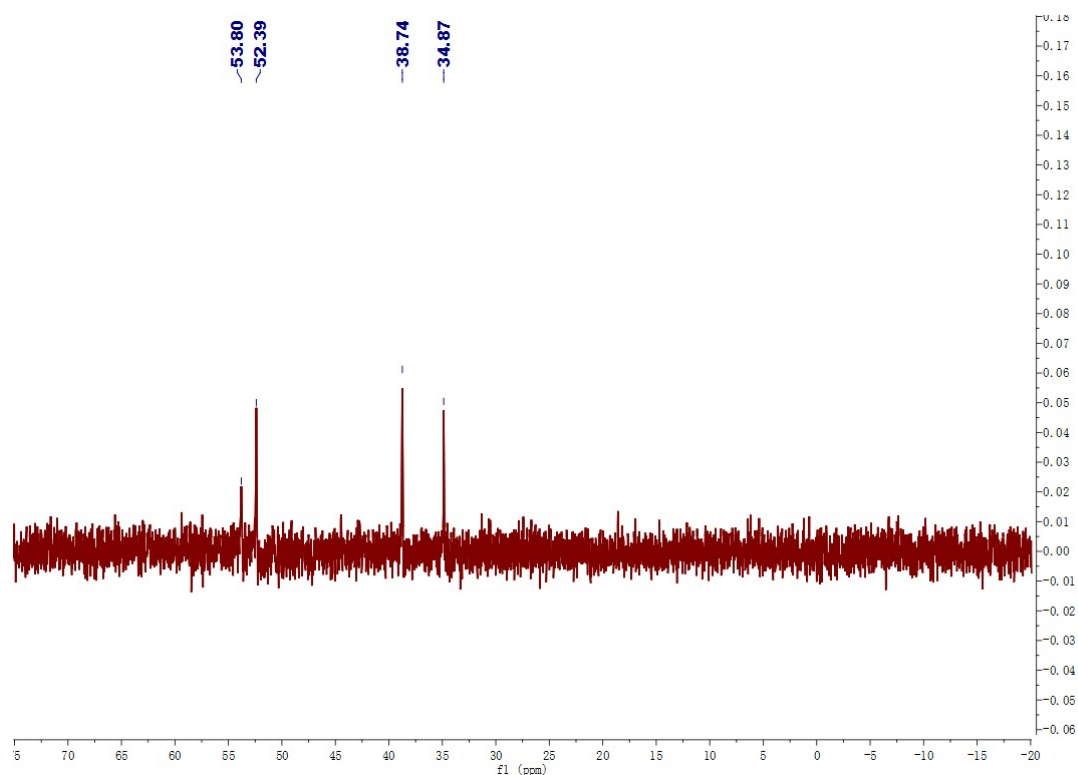


¹H NMR spectrum (400 MHz, CDCl₃, 298K) of *o*-TPEA.

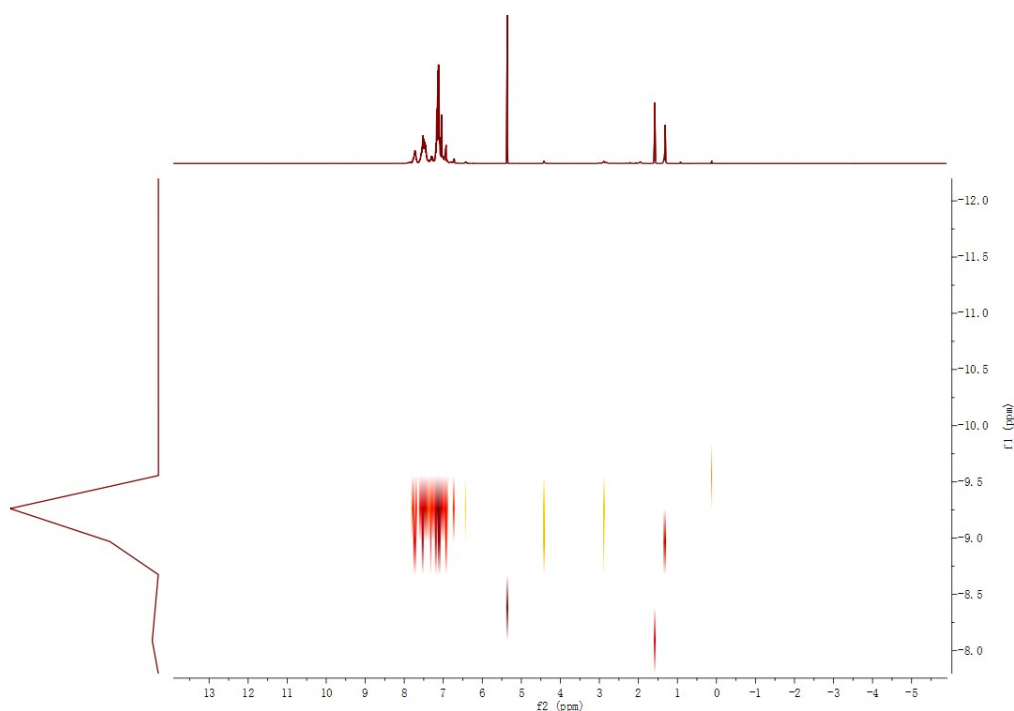


¹³C NMR spectrum (100 MHz, CDCl₃, 298K) of *o*-TPEA.

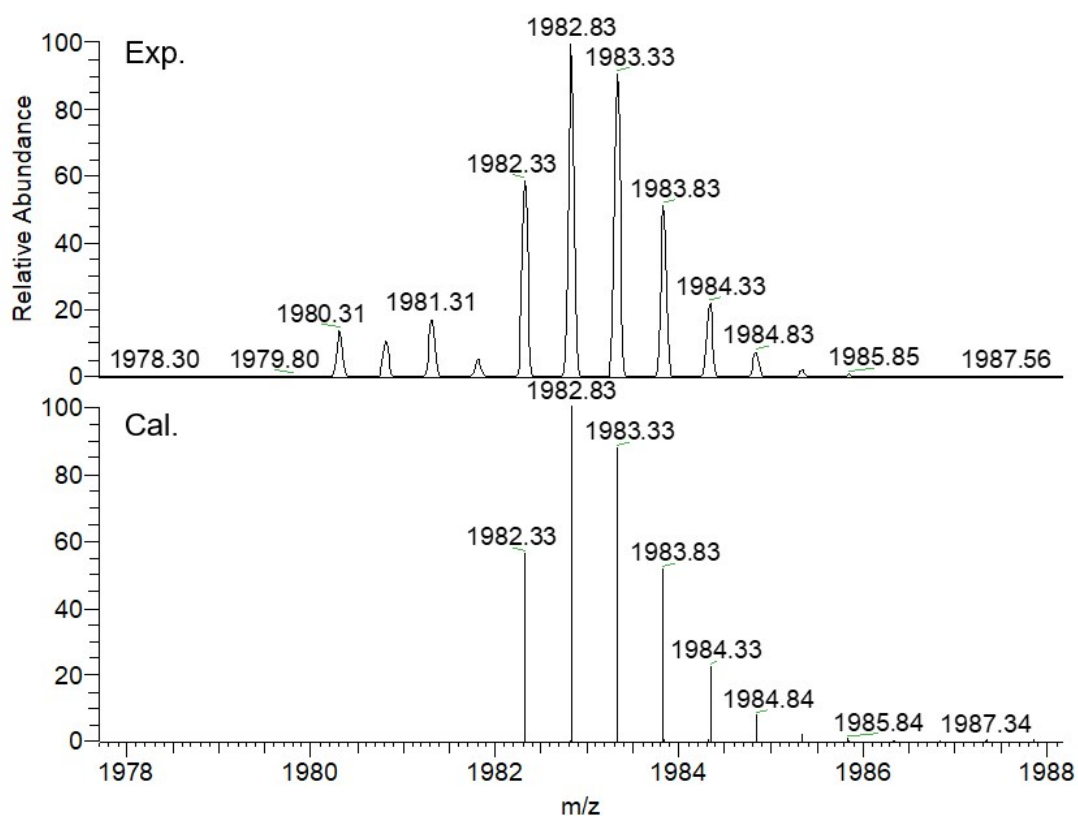
Synthesis of 1a. The initial cluster $[\text{Au}_8(\text{dppp})_4](\text{NO}_3)_2$ was synthesized as the reported method^[15]. MeONa (90.7 mg, 1.68 mmol), 2-(trimethylsilyl)ethynyl-4-(1,2,2-triphenylethenyl)-phenylamine (8.3 mg, 22.4 μmol) and 30 mL MeOH were added into a 100 mL flask. Then 2 mL MeOH solution of $[\text{Au}_8(\text{dppp})_4](\text{NO}_3)_2$ (18.8 mg, 5.6 μmol , 1 eq.) were added into the flask and the solution was stirred for 24h at 310 K. The solution turned from purple to red after 24 h. 50 mL H_2O was added into the solution and the mixture was extracted with 10 mL CH_2Cl_2 for three times. The crude product was collected by adding diethyl ether into the condensed CH_2Cl_2 solution of **1a**. Red crystals of **1a** were obtained by slow diffusion of diethyl ether into the concentrated $\text{CH}_2\text{Cl}_2/\text{MeOH}$ (v/v = 1:1) mixed solution of **1a**. Yield: 31% (7.1 mg, 1.7 μmol). Elemental analysis for $[\text{Au}_8(\text{dppp})_4(o\text{-TPEA})_2](\text{NO}_3)_2(\text{CH}_2\text{Cl}_2)_3$ ($\text{C}_{167}\text{H}_{150}\text{Au}_8\text{N}_2\text{O}_6\text{P}_8\text{Cl}_6$), found (calcd): C, 46.84 (46.46); H, 3.29 (3.50); N, 0.58 (0.65). ESI-MS, found (calcd): 1982.83 (1982.33) ($[\text{M}-2\text{NO}_3]^{2+}$).



^{31}P NMR spectrum (400 MHz, CD_2Cl_2 , 298K) of **1a**.



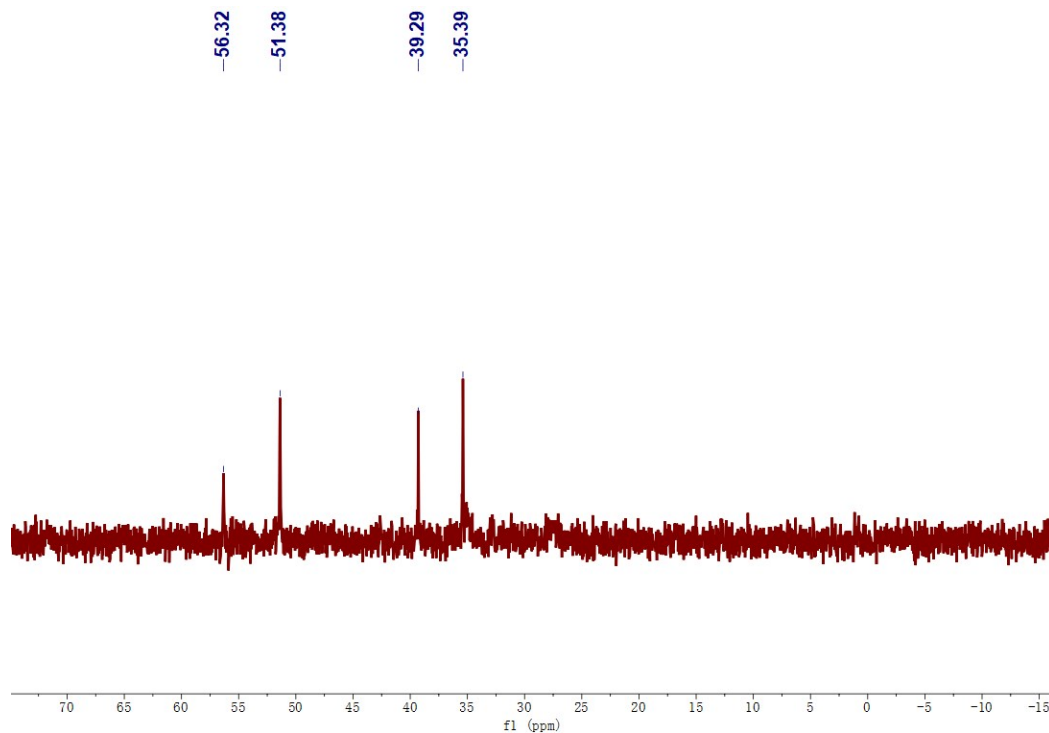
DOSY ^1H NMR spectrum (600 MHz, CD_2Cl_2 , 298K) of **1a**.



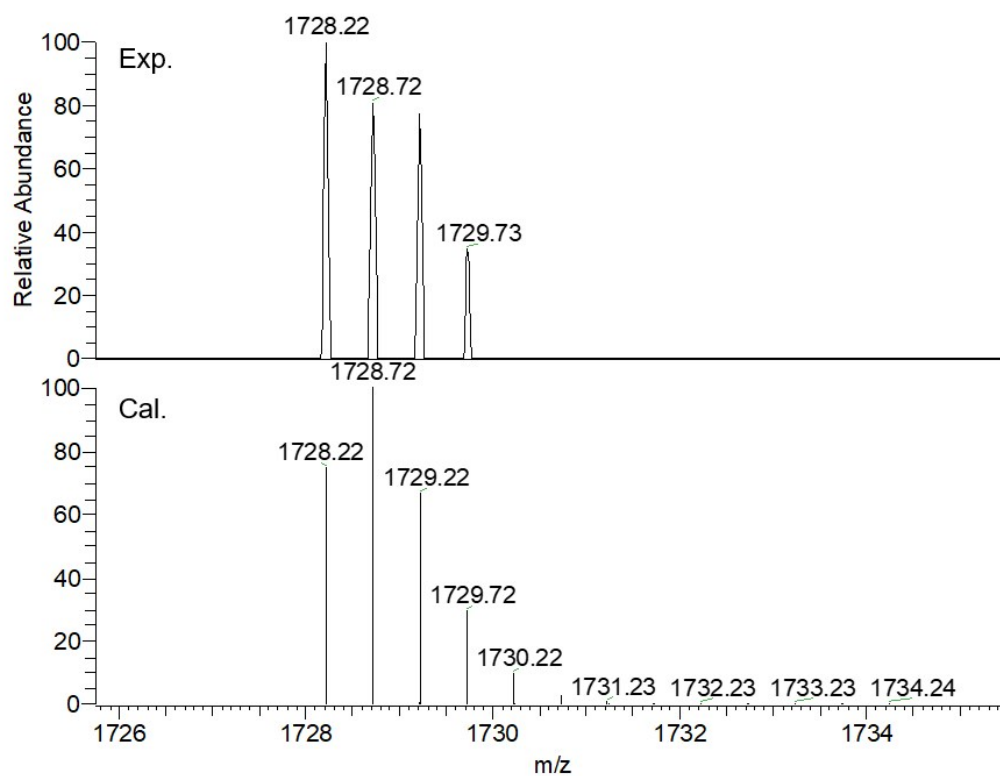
ESI-MS spectrum of **1a** (Experimental and calculated $[\text{M}-2\text{NO}_3]^{2+}$ signals).

Synthesis of 1b. The reaction was performed following the procedure of **1a** described above, replacing 2- (trimethylsilyl)ethynyl-4-(1,2,2-triphenylethenyl)-phenylamine by

2-ethynyl-benzenamine (2.6 mg, 22.4 μmol). Crystals of **1b** were obtained by the yield of 47% (9.3 mg, 2.6 μmol). Elemental analysis for $[\text{Au}_8(\text{dppp})_4(o\text{-EBA})_2](\text{NO}_3)_2(\text{CH}_2\text{Cl}_2)_2$ ($\text{C}_{126}\text{H}_{130}\text{Au}_8\text{N}_2\text{O}_6\text{P}_8\text{Cl}_4$), found (calcd): C, 40.85 (40.23); H, 3.28 (3.48); N, 1.31 (1.49). ESI-MS, found (calcd): 1728.72 (1728.22) ($[\text{M}-2\text{NO}_3]^{2+}$).

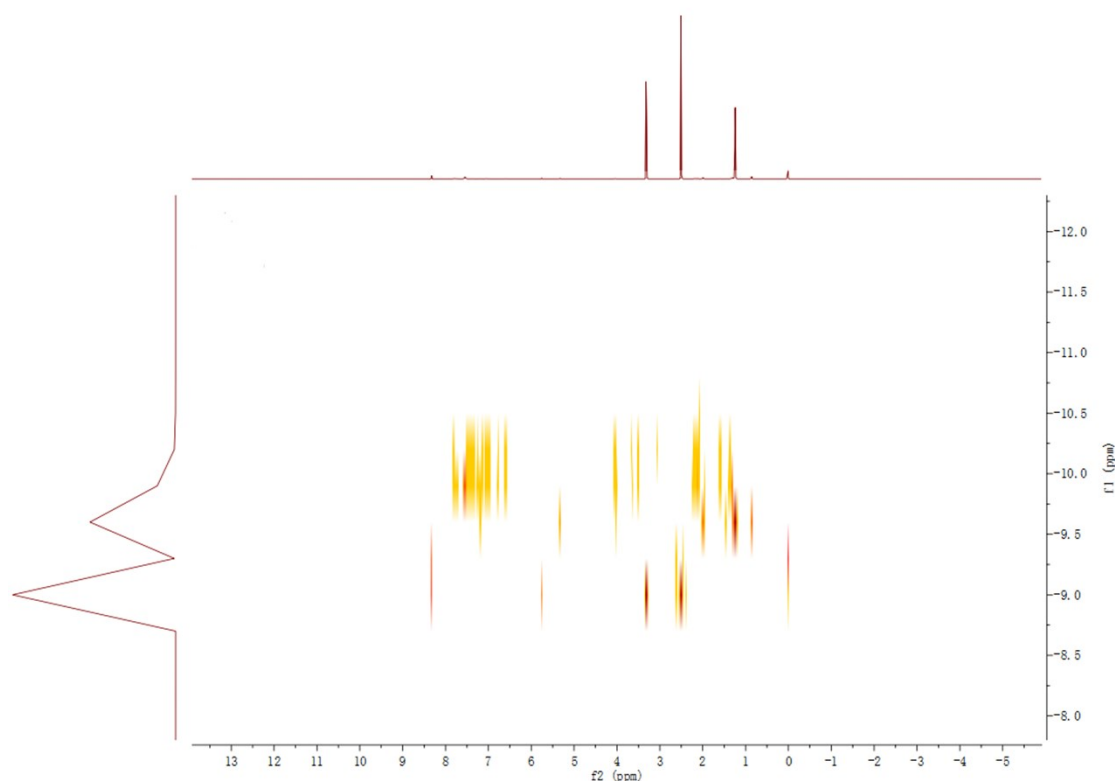


^{31}P NMR spectrum (400 MHz, CD_2Cl_2 , 298K) of **1b**.



ESI-MS spectrum of **1b**. (Experimental and calculated $[\text{M}-2\text{NO}_3]^{2+}$ signals)

Synthesis of P1a. At room temperature, 2,4-TDI (2.1 mg, 10.0 μ M) and 1,8-octanediol (1.2 mg, 8.0 μ M) were added into a 10mL sealing tube and then dissolved in 2 mL anhydrous THF. 1mL anhydrous dichloromethane (DCM) solution of **1a** (4.1 mg, 1.0 μ M) was slowly injected into the sealing tube under stirring. After reaction at 313K for 24h, 1mL anhydrous DCM solution of mPEG2000 (4.8 mg, 2.4 μ M) was added into the tube. After stirring for further 24 h, red precipitate appeared at the bottle of the sealing tube and the solution turned colourless. The product **P1a** was collected by filtration and was subject to washing via DCM (3 \times 5 mL), MeOH (3 \times 5 mL) and H₂O (3 \times 5 mL). Inductive coupled plasma optical emission spectrometer (ICP-OES), mass fraction of Au element: 19.8%.



DOSY ¹H NMR spectrum (600 MHz, DMSO-*d*₄, 298K) of **P1a**.

X-ray crystallography

Single-crystal X-ray data for gold cluster complexes **1a** (CCDC-2067717) and **1b** (CCDC-2067718) were collected at 173 K with Cu K α radiation ($\lambda = 1.54178$ Å) on a Rigaku Oxford Diffraction SuperNova diffractometer. The selected crystal was mounted onto a nylon loop by poly-isobutene and enveloped in a low-temperature (173K) stream of dry nitrogen gas during data collection. The absorption corrections were applied using multi-scan methods. All structures were solved by direct methods, and non-hydrogen atoms were located from difference Fourier maps. Non-hydrogen atoms were subjected to anisotropic refinement by full-matrix least-squares on F^2 using the SHELXTL program^[2] and Olex² program^[3] unless otherwise noted. All figures were drawn by using the X-seed program.^[4] Crystal data for **1a**: C₁₆₄H₁₄₄Au₈N₂P₈, $M = 3457.67$, monoclinic, space group P -1, $a = 18.7088(7)$ Å, $b = 16.0003(7)$ Å, $c =$

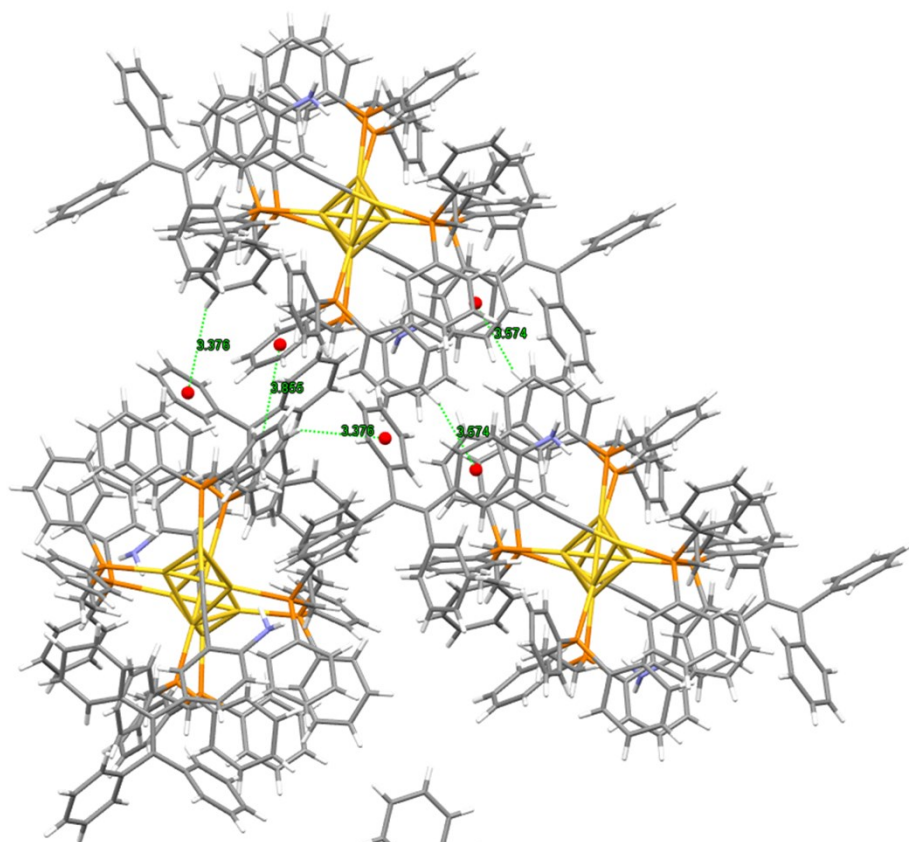
26.2937(12) Å, $V = 7835.3(6)$ Å³, $Z = 2$, $T = 173$ K, $D_c = 1.681$ g/cm³. The structure, refined on F^2 , converged for 7 459 unique reflections ($R_{\text{int}} = 0.0822$) and 13 109 observed reflections with $I > 2\sigma(I)$ to give $R_1 = 0.1457$ and $wR_2 = 0.3487$ and a goodness-of-fit = 1.064. Crystal data for **1b**: $C_{124}H_{126}Au_8N_2P_8$, $M = 3966.34$, monoclinic, space group $P 21/c$, $a = 17.5317(3)$ Å, $b = 19.3738(3)$ Å, $c = 20.9396(3)$ Å, $V = 6364.15(18)$ Å³, $Z = 2$, $T = 173$ K, $D_c = 1.810$ g/cm³. The structure, refined on F^2 , converged for 20 380 unique reflections ($R_{\text{int}} = 0.0875$) and 24 899 observed reflections with $I > 2\sigma(I)$ to give $R_1 = 0.0795$ and $wR_2 = 0.2265$ and a goodness-of-fit = 1.021. Positive residual densities on heavy metal ions are acceptable^[9, 10].

Computational details

Theoretical calculations of model clusters were performed using the Gaussian 09 program. Structures of **1a-1c** for calculation were built up on the basis of corresponding single-crystal structures. The Becke three-parameter hybrid functional accompanied by the Lee–Yang–Parr correlation functional (B3LYP)^[5] was employed in the TD-DFT calculation without any symmetry constraints on molecular structures. The basis sets of def2-DZVP^[6] and def2-SVP^[7] were applied for gold and the other atoms respectively. Sixty singlet states ($n_{\text{state}} = 60$, singlet) are chosen in the calculations of the UV-vis absorption of 1a-1c-based model clusters. The root is set as 1 in all of the TD-DFT calculations. Data for orbital composition analysis with Mulliken partition are from Gaussian 09 calculations and processed with Multiwfn software^[8]. Plots of theoretically calculated UV-vis and CD spectra are obtained by using Multiwfn software.

Supporting figures

(a)



(b)

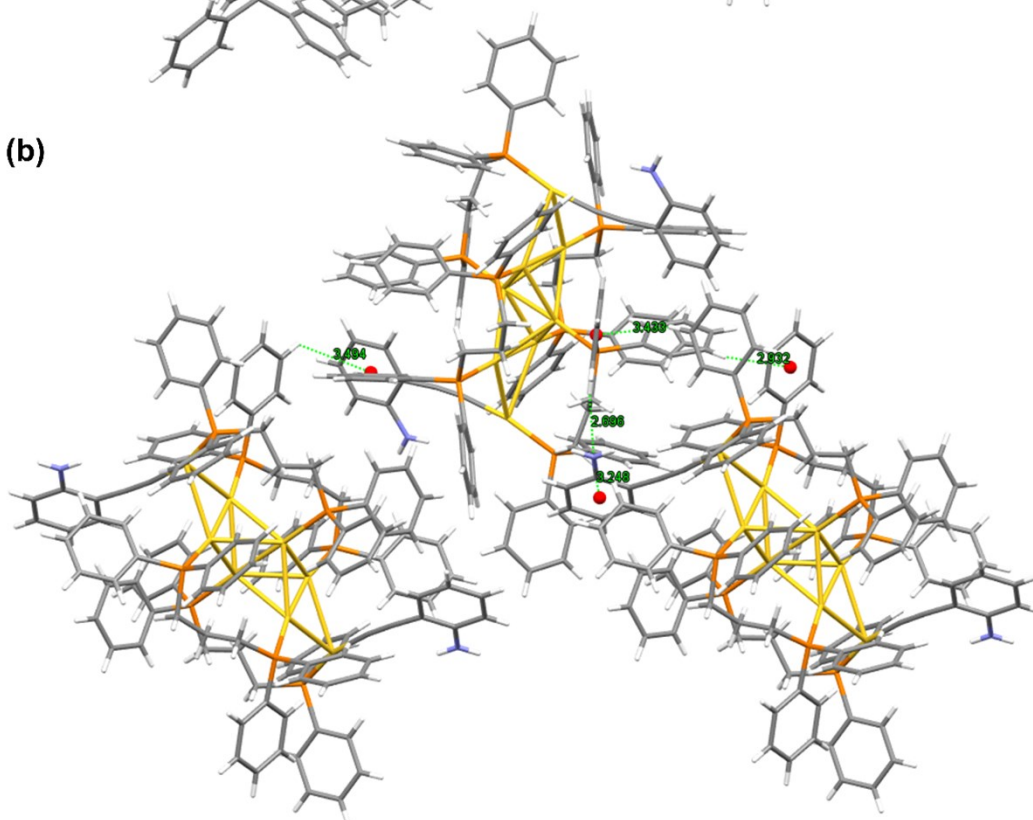


Fig. S1 Packing modes in crystal structures of (a) **1a** and (b) **1b**.

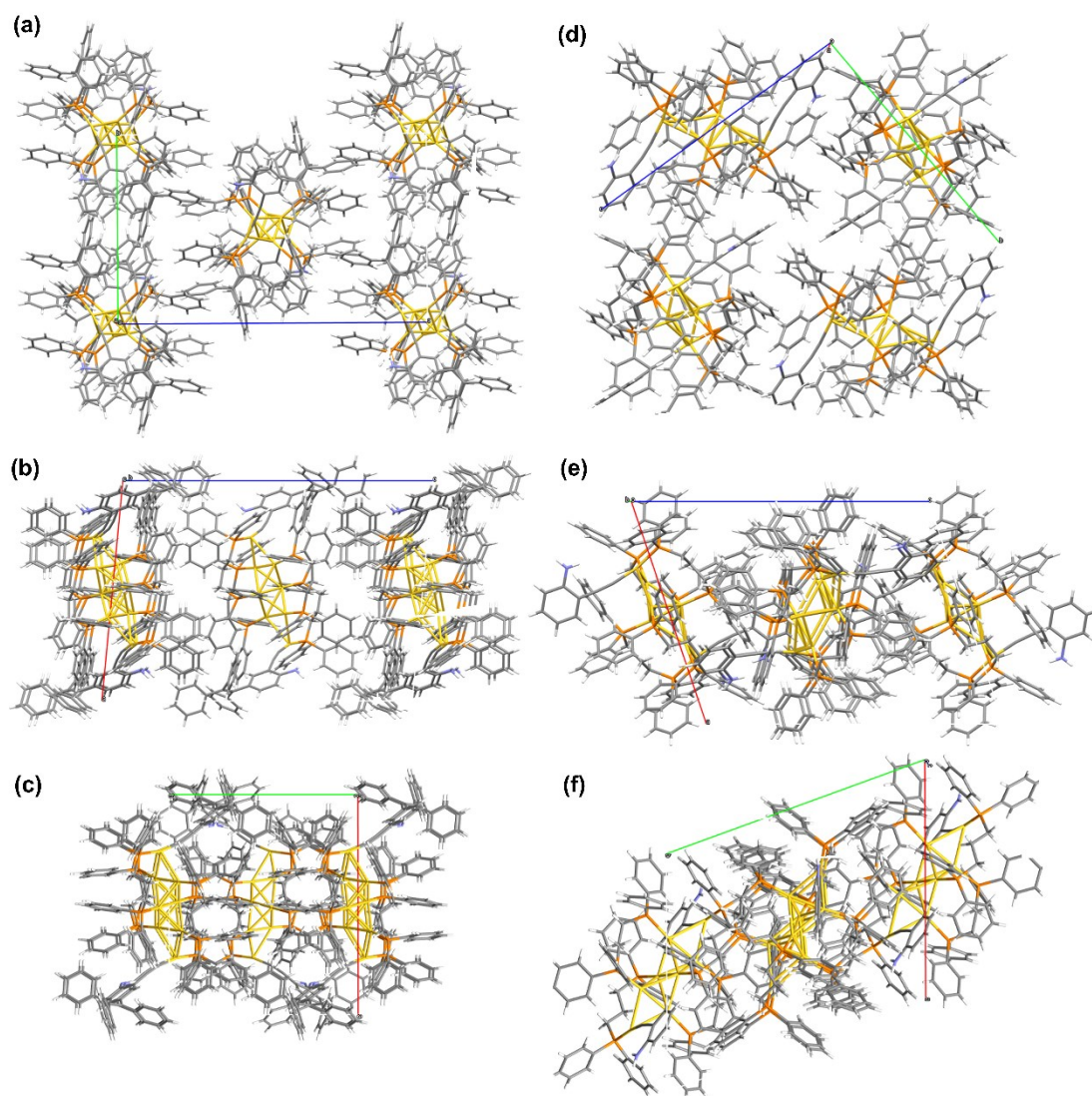


Fig. S2 Packing modes of crystal structures of (a-c) **1a** and (d-f) **1b** in different axes.

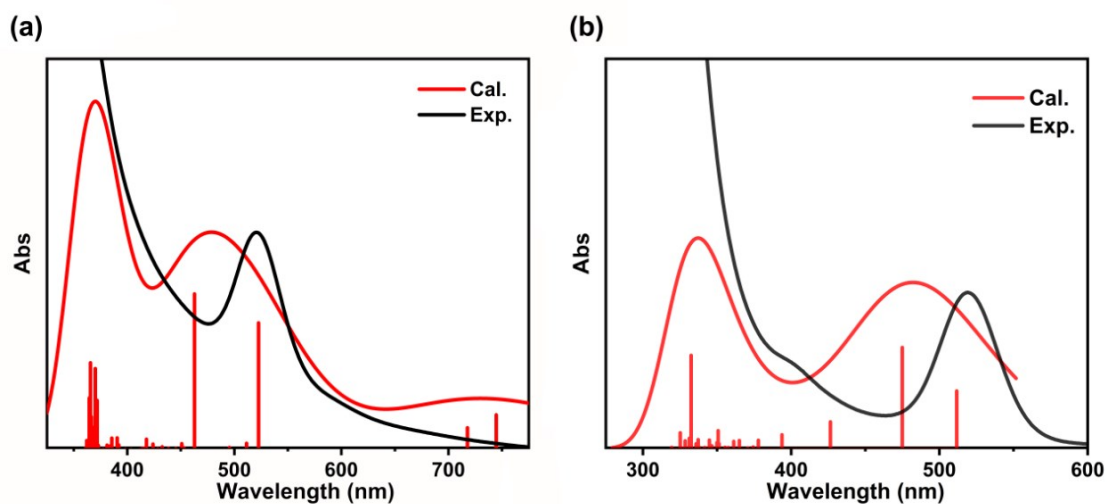


Fig. S3 Theoretical absorption spectra (red lines) of (a) **1a** and (b) **1b**. Experimental absorption spectra of them (black lines) are shown for comparison.

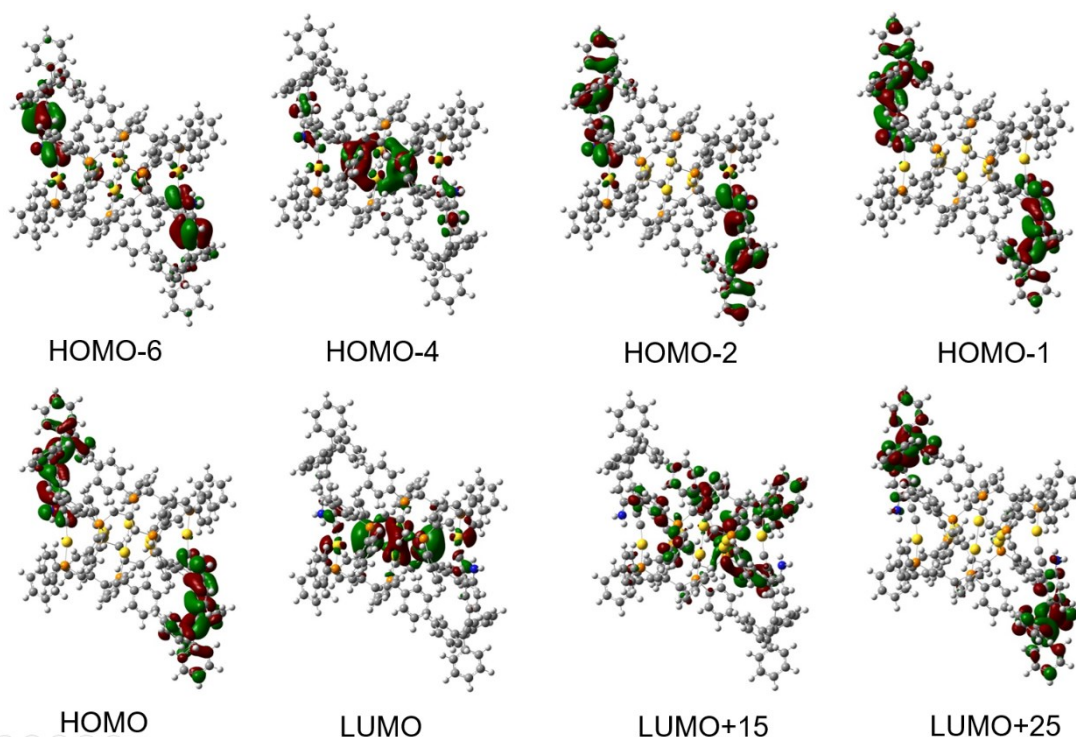


Fig. S4 Selected molecular orbitals of **1a**.

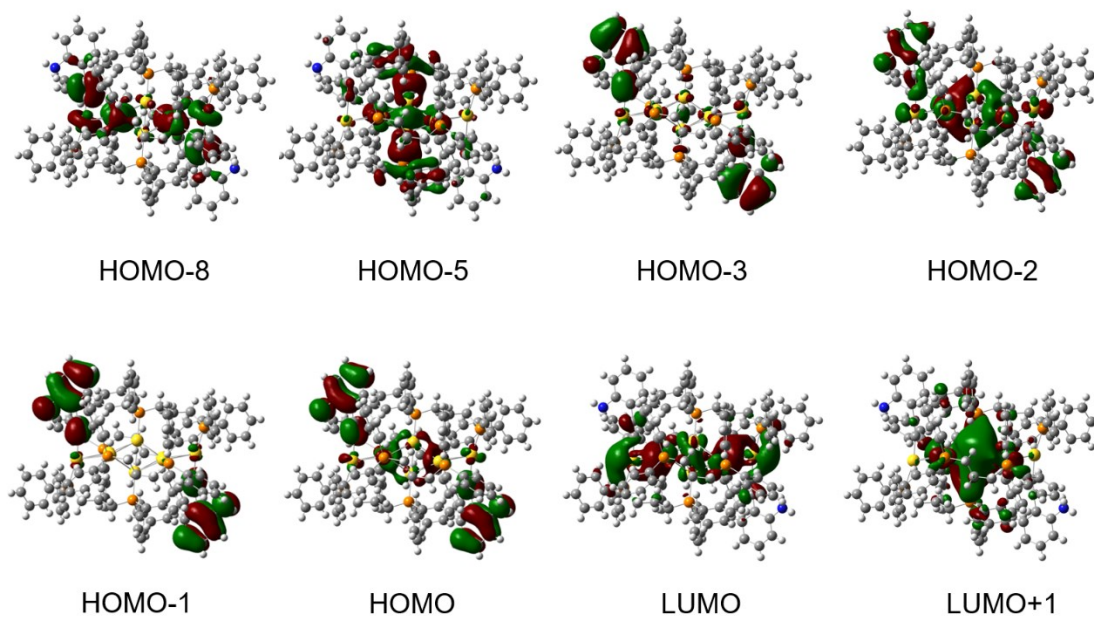


Fig. S5 Selected molecular orbitals of **1b**.

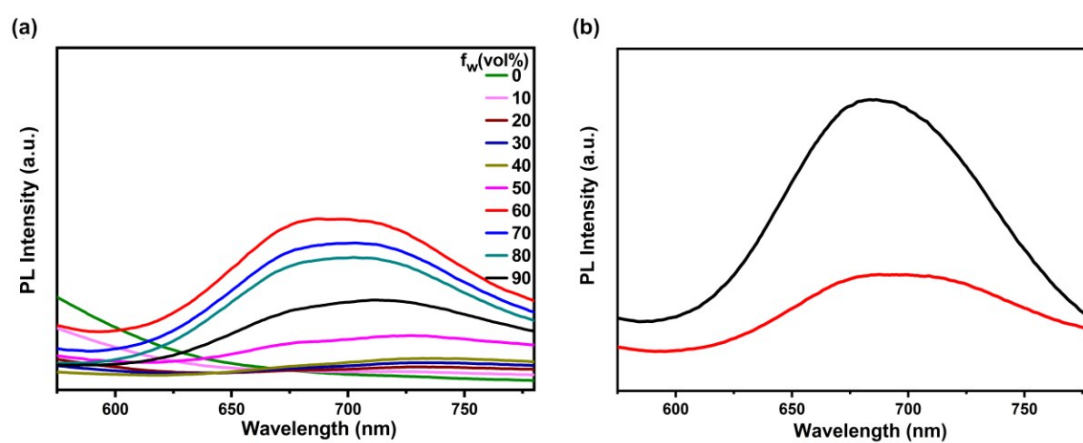


Fig. S6 (a) PL spectra of **1a** ($c = 20 \mu\text{M}$) in MeOH/H₂O mixed solvent ($\lambda_{\text{ex}} = 420 \text{ nm}$). (b) PL of **1a** ($c = 20 \mu\text{M}$) in 60% H₂O-MeOH mixed solvent. Black line: $\lambda_{\text{ex}} = 520 \text{ nm}$; Red line: $\lambda_{\text{ex}} = 420 \text{ nm}$.

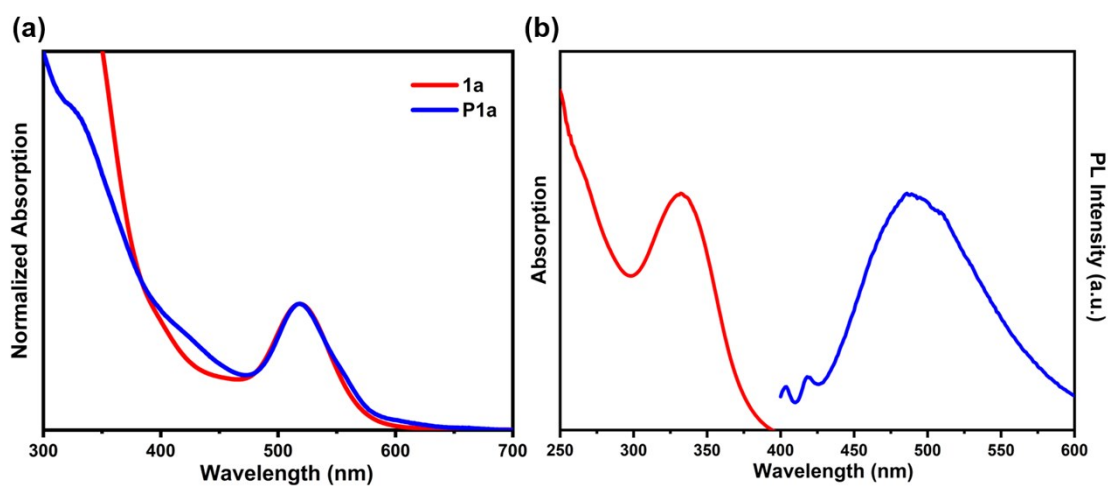
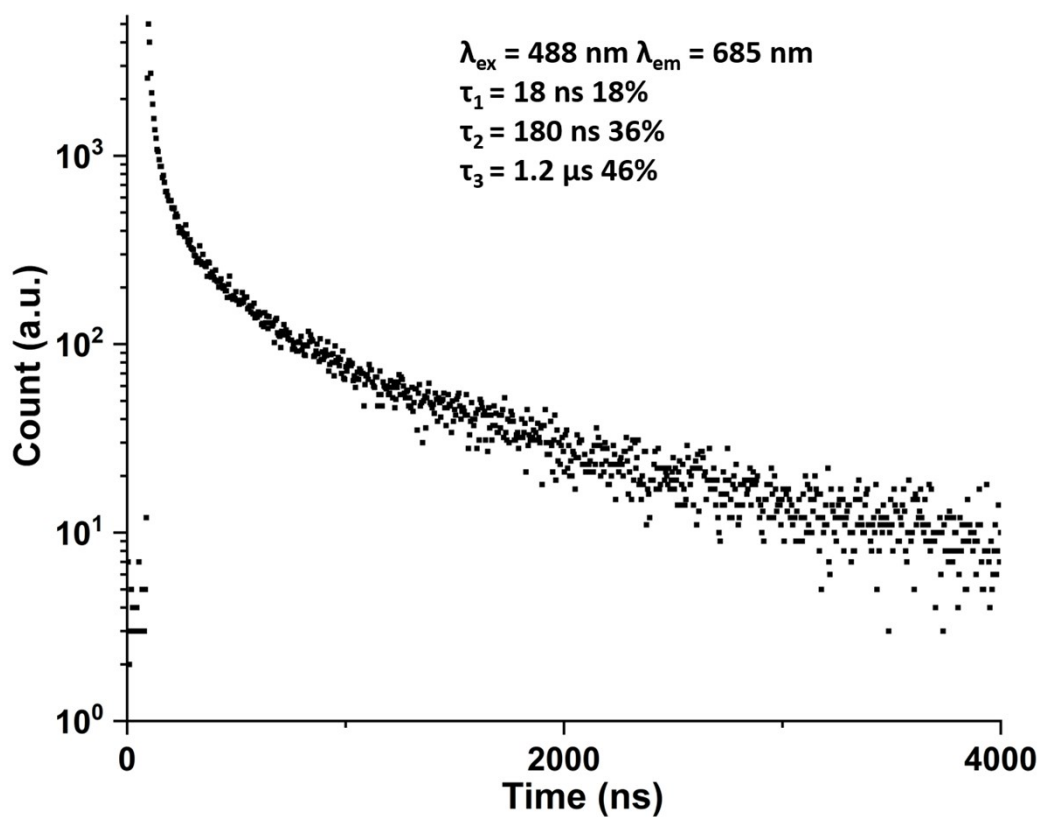


Fig. S7 (a) Absorption spectra of **P1a** in water and **1a** in methanol ($c = 10 \mu\text{M}$). (b) Absorption (red line) and emission (blue line, $\lambda_{\text{ex}} = 330 \text{ nm}$) spectrum of *o*-TPEA in 90% H₂O-Methanol mixed solvent ($c = 10 \mu\text{M}$).



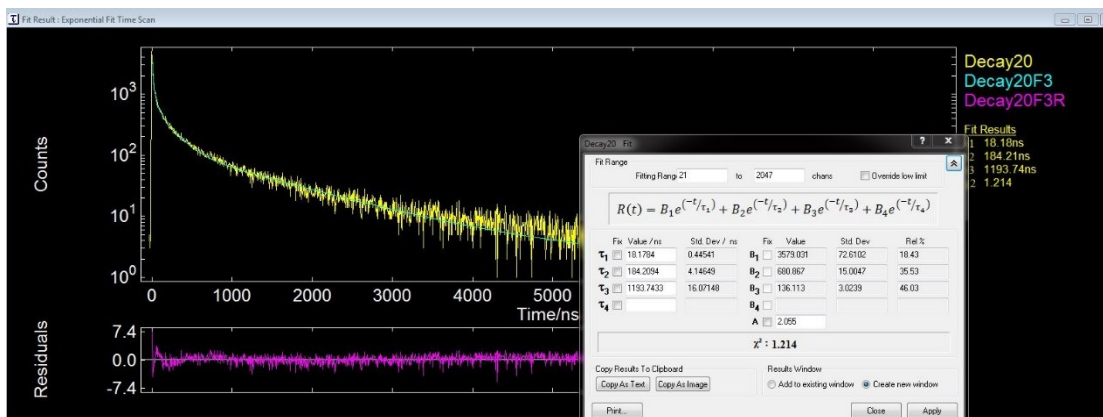


Fig. S8 Emission lifetime curves collected at room temperature and corresponding fits for **1a** in 90% H₂O/MeOH mixed solvent (20 μ M). λ_{ex} = 488 nm, λ_{em} = 685 nm.

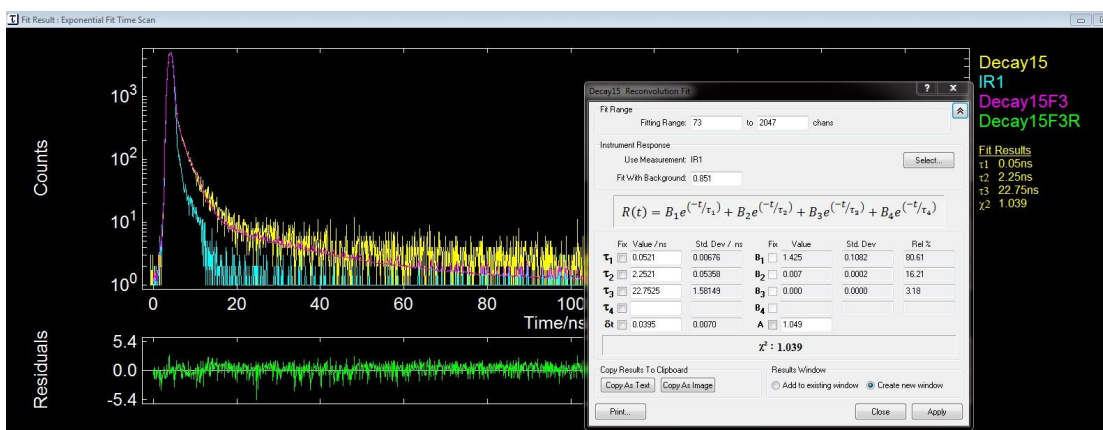
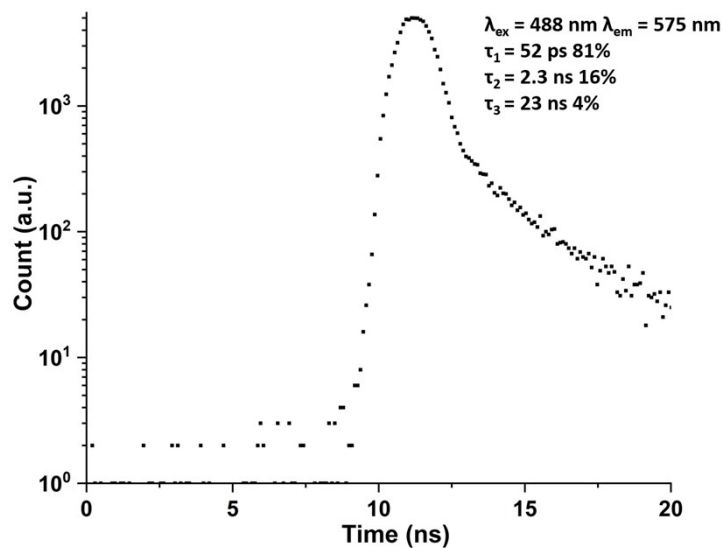


Fig. S9 Emission lifetime curves collected at room temperature and corresponding fits for **1b** in 90% H₂O/MeOH mixed solvent (20 μ M). λ_{ex} = 488 nm, λ_{em} = 575 nm.

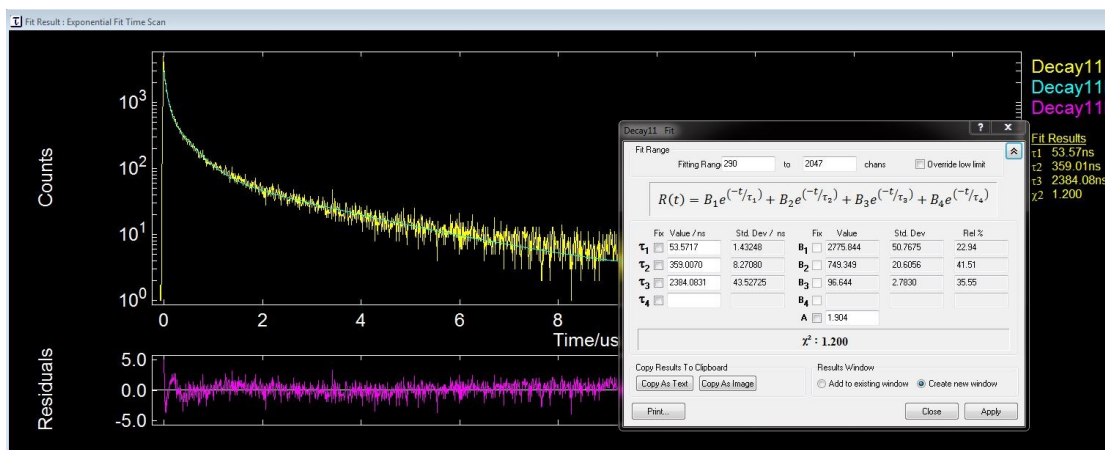
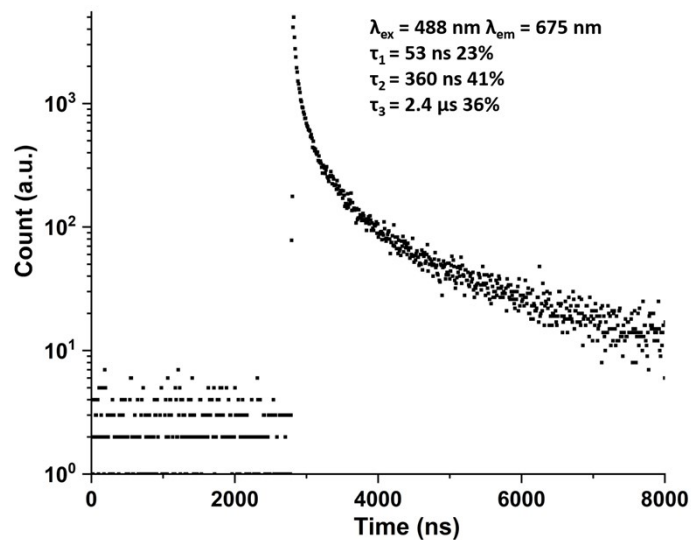
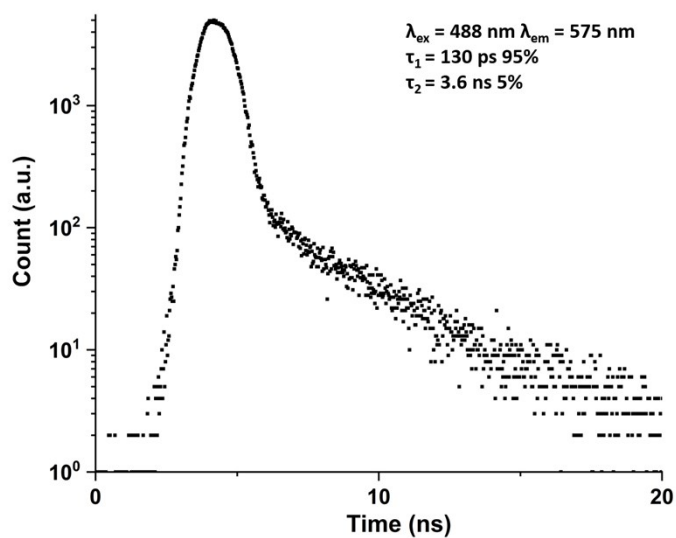


Fig. S10 Emission lifetime curves collected at room temperature and corresponding fits for **1b** in 90% H₂O/MeOH mixed solvent (20 μ M). $\lambda_{\text{ex}} = 488 \text{ nm}$, $\lambda_{\text{em}} = 675 \text{ nm}$.



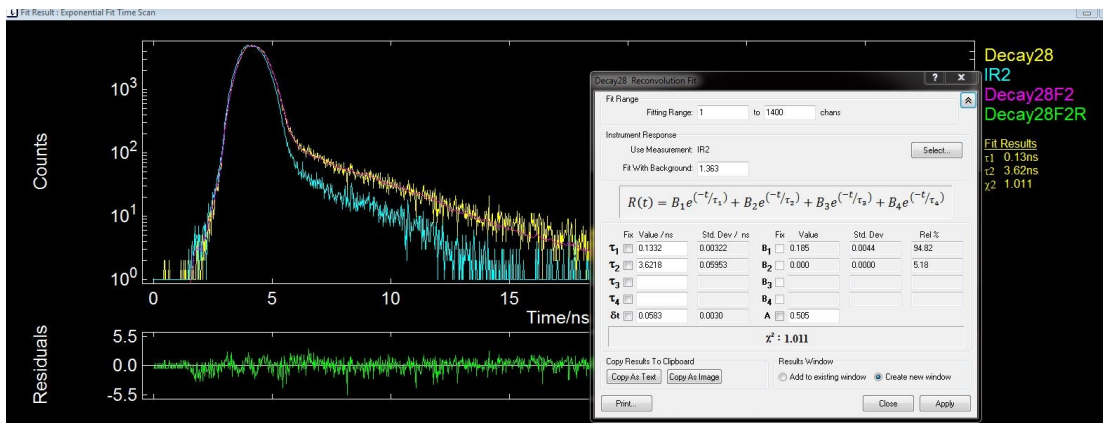


Fig. S11 Emission lifetime curves collected at room temperature and corresponding fits for **1c** in 90% H₂O/MeOH mixed solvent (20 μ M). λ_{ex} = 488 nm, λ_{em} = 575 nm.

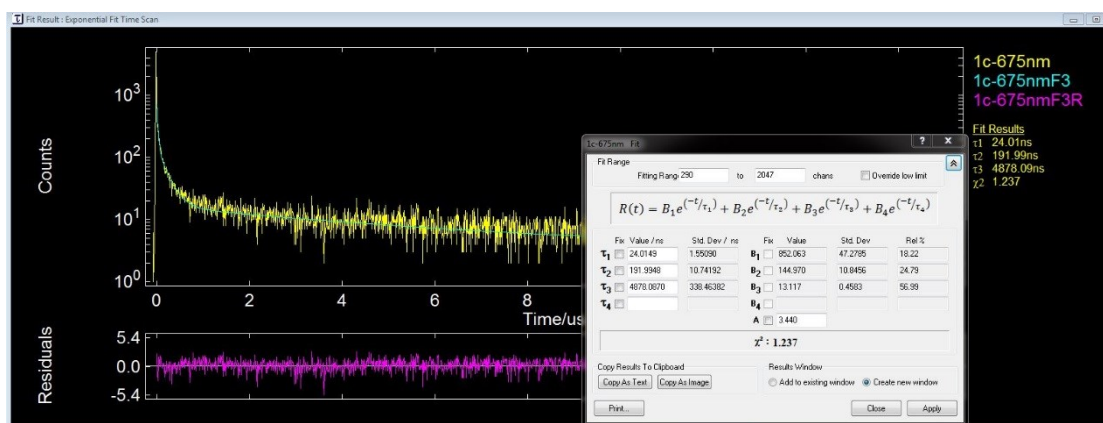
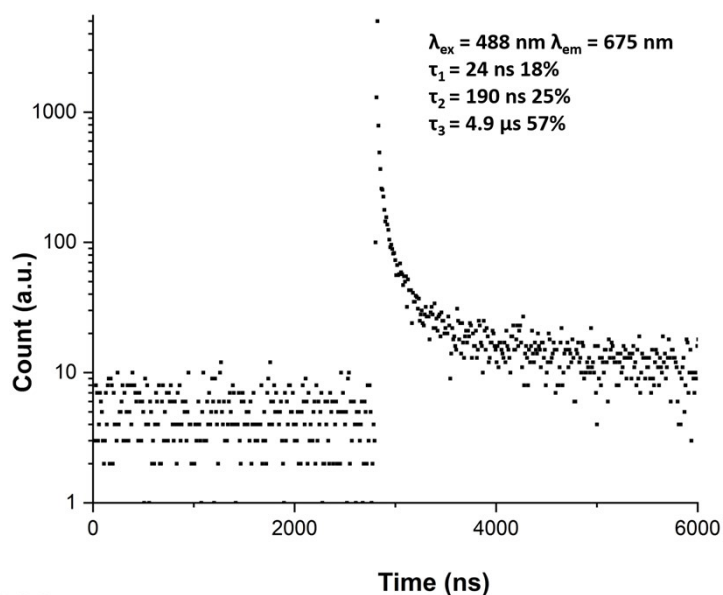


Fig. S12 Emission lifetime curves collected at room temperature and corresponding fits for **1c** in 90% H₂O/MeOH mixed solvent (20 μ M). λ_{ex} = 488 nm, λ_{em} = 675 nm.

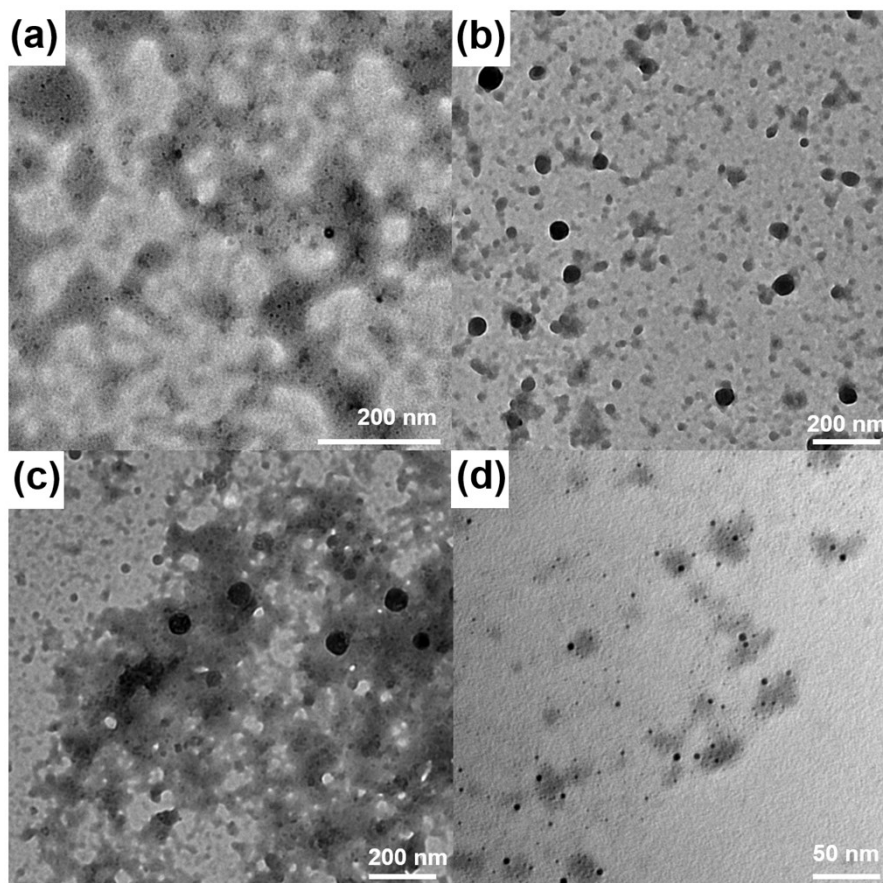


Fig. S13 TEM image of **1a** in different MeOH/H₂O solvent. (a) $f_w = 0$, (b) $f_w = 60\%$, and (c) $f_w = 90\%$. (d) TEM image of **P1a** in water.

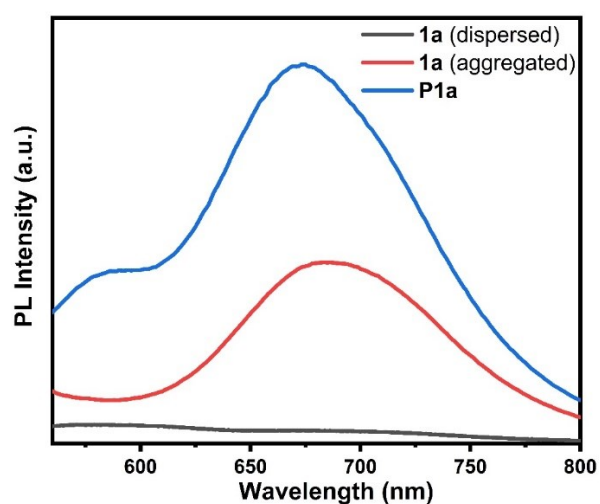


Fig. S14 Photoluminescent spectra of dispersed **1a** (in MeOH), aggregated **1a** (in 60% H₂O-MeOH mixed solvent) and **P1a** (in H₂O). The concentrations are normalized as 20 μM counted by the Au₈ cluster in these three samples.

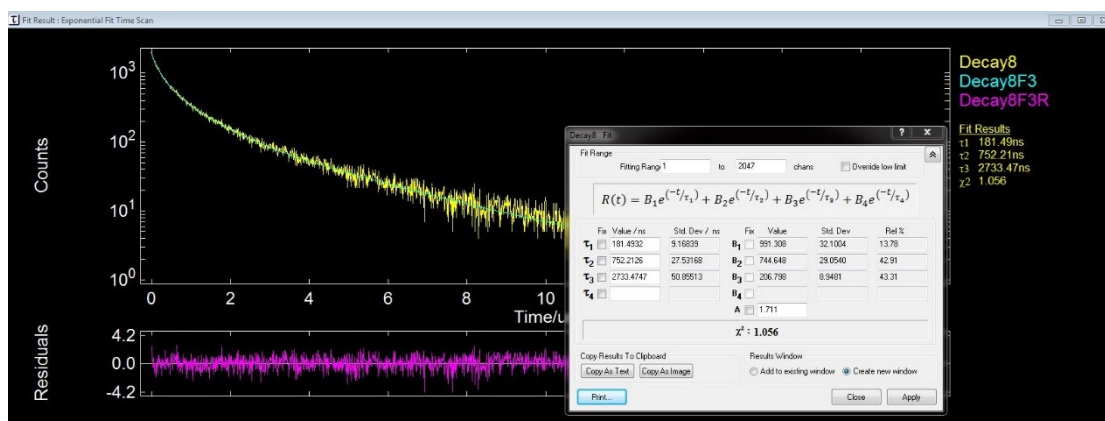
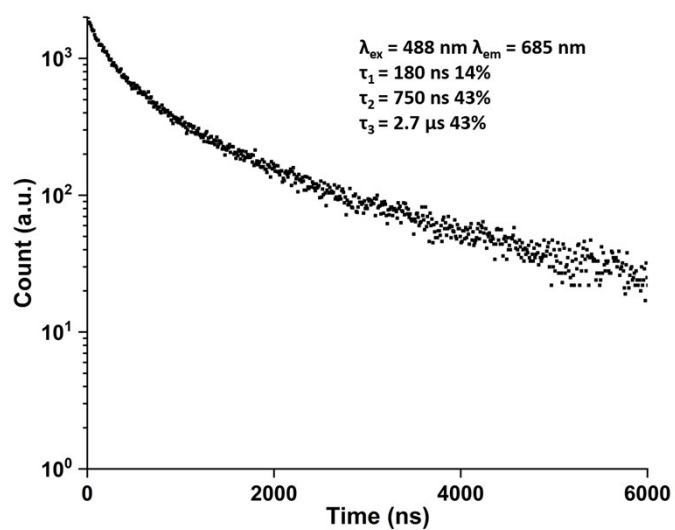


Fig. S15 Emission lifetime curves collected at room temperature and corresponding fits for P1a in H₂O (10 μ M). $\lambda_{\text{ex}} = 488 \text{ nm}$, $\lambda_{\text{em}} = 685 \text{ nm}$.

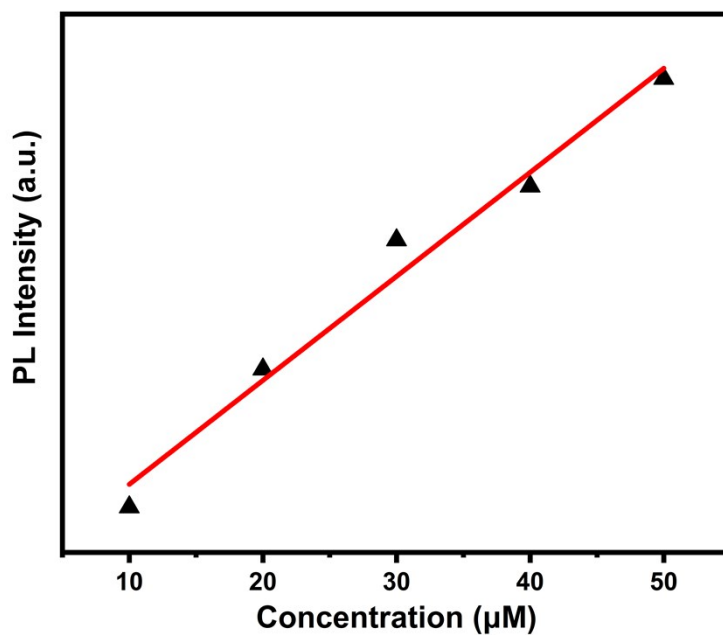


Fig. S16 PL intensity of P1a in different concentrations (in water).

Table S1 Bond length and bond angles in **1a**, **1b** and **1c**.

Bond lengths (Å) or bond angles (°)	1a	1b	1c
Au1-Au2	3.075(6)	3.116(3)	3.071(9)
Au1-Au4'	3.026(9)	3.006(3)	2.970(3)
Au2-Au3'	2.859(8)	2.838(3)	2.841(1)
Au2-Au4'	2.637(9)	2.653(8)	2.650(4)
Au3-Au3'	2.635(4)	2.601(9)	2.647(9)
Au3-Au4	2.821(5)	2.850(1)	2.792(0)
Au1-C1	1.970(5)	1.942(3)	-
C1-C2	1.180(8)	1.206(1)	-
P1-P3	4.944(9)	5.423(2)	4.982(6)
P2-P4	4.882(9)	4.920(1)	4.810(1)
Au1-C1-C2	167.18	170.27	-
Au1-Au2Au4'-Au3'	163.61	163.51	163.15

Table S2 Orbital transitions of **1a**.

Wavelength (nm)	Dominant transition	Mechanism
519.8	HOMO-2 → LUMO	LMCT
460.7	HOMO-4 → LUMO, HOMO-6 → LUMO	MMCT, LMCT
377.3	HOMO-1 → LUMO+15~28	$\pi \rightarrow \pi^*$

Table S3 Orbital transitions of **1b**.

Wavelength (nm)	Dominant transition	Mechanism
505.14	HOMO-1 → LUMO	LMCT
474.61	HOMO-2 → LUMO	LMCT/MMCT
332.3	HOMO-8 → LUMO, HOMO-3/HOMO-5 → LUMO+1	LMCT/ MMCT

Table S4 Atomic contributions of **1a**.

MOs	Au	dppp	<i>o</i> -TPEA
HOMO-4	51.69%	24.86%	23.50%
HOMO-3	4.04%	3.41%	92.56%
HOMO-2	8.70%	3.03%	88.28%
HOMO-1	1.48%	7.67%	90.85%
HOMO	1.40%	0.36%	98.24%
LUMO	72.66%	19.89%	7.46%
LUMO+1	60.66%	39.00%	0.35%
LUMO+2	47.90%	51.66%	0.44%
LUMO+3	37.75%	61.32%	0.93%
LUMO+15	11.80%	86.34%	1.86%
LUMO+16	11.19%	86.97%	1.84%

LUMO+18	8.88%	89.89%	1.23%
LUMO+19	5.94%	86.83%	7.23%
LUMO+21	5.33%	64.91%	29.76%
LUMO+22	6.20%	69.26%	24.54%
LUMO+23	6.76%	61.20%	32.03%
LUMO+25	4.51%	89.12%	6.38%
LUMO+26	9.97%	66.20%	23.84%
LUMO+27	1.89%	20.27%	77.84%

Table S5 Atomic contributions of **1b**.

MOs	Au	dppp
HOMO-8	32.24%	32.39%
HOMO-5	30.90%	63.00%
HOMO-3	8.52%	7.02%
HOMO-2	51.08%	17.53%
HOMO-1	3.67%	1.08%
HOMO	19.57%	6.18%
LUMO	71.74%	18.58%
LUMO+1	60.44%	36.82%

Table S6 life time of **1a~c** and **P1a**.^a

Cluster	λ_{ex} (nm)	λ_{em} (nm)	lifetime τ_1	τ_2	τ_3	Q.Y. %
1a	488	685 ^b	18 ns (18%)	180 ns (36%)	1.2 μ s (46%)	0.3
1b	488	575 ^c	52 ps (81%)	2.3 ns (16%)	23 ns (4%)	-
		675 ^b	53 ns (23%)	360 ns (41%)	2.4 μ s (36%)	0.1
1c	488	575 ^c	130 ps (95%)	3.6 ns (5%)	-	-
		675 ^b	24 ns (18%)	190 ns (25%)	4.9 μ s (57%)	0.1
P1a	488	685 ^d	180 ns (14%)	750 ns (43%)	2.7 μ s (43%)	0.7

^a Unless otherwise stated, lifetime data were obtained at 25°C, c = 10 μ M, λ_{ex} = 488 nm, and the spectra were monitored at λ_{em} . ^b In 90% H₂O-MeOH mixed solvent. ^c In MeOH. ^d In H₂O.

Table S7 Diffusion coefficients, and calculated and measured sizes of **1a** and **P1a** based on DOSY measurements.

Compounds	Diffusion coefficient/ $\text{m}^2 \cdot \text{s}^{-1}$	Calculated diameter/ \AA	Diameter in crystal structures/ \AA
1a	6.833×10^{-10}	14.51	27.09
P1a	1.179×10^{-10}	18.5	-

References

- 1 Y. Kamei, Y. Shichibu, K. Konishi, *Angew. Chem., Int. Ed.*, 2011, **50**, 7442.
- 2 G. M. Sheldrick, *Acta Crystallogr., Sect. A: Found. Crystallogr.*, 2008, **64**, 112.
- 3 O. V. Dolomanov, L. J. Bourhis, R. J. Gildea, J. A. K. Howard and H. Puschmann, *J. Appl. Crystallogr.*, 2009, **42**, 339.
- 4 J. L. Atwood and L. J. Barbour, *Cryst. Growth Des.*, 2003, **3**, 3.
- 5 (a) A. D. Becke, *J. Chem. Phys.*, 1993, **98**, 5648; (b) C. Lee, W. Yang and R. G. Parr, *Phys. Rev. B*, 1988, **37**, 785.
- 6 F. Weigend, R. Ahlrichs, *Phys. Chem. Chem. Phys.*, 2005, **7**, 3297.
- 7 A. Schafer, H. Horn, R. J. Ahlrichs, *Chem. Phys.*, 1992, **97**, 2571.
- 8 T. Lu and F. Chen, *J. Comput. Chem.*, 2012, **33**, 580.
- 9 I. Brekalo, C. M. Knae, A. N. Ley, J. R. Ramirez, T. Friscic, K. T. Holman, *J. Am. Soc. Chem.*, 2018, **140**, 10104.
- 10 C. M. R. Wright, T. J. Williams, Z. R. Turner, J.-C. Buffet, D. O'Hare, *Inorg. Chem. Front.*, 2017, **4**, 1048.